Food Chemistry 241 (2018) 317–327

Contents lists available at ScienceDirect

Food Chemistry

journal homepage: www.elsevier.com/locate/foodchem

Encapsulating anthocyanins from *Hibiscus sabdariffa* L. calyces by ionic gelation: Pigment stability during storage of microparticles

Sílvia C.S.R. de Moura[a,c,*], Carolina L. Berling[b], Sílvia P.M. Germer[c], Izabela D. Alvim[d], Míriam D. Hubinger[a]

[a] Department of Food Engineering, School of Food Engineering, University of Campinas, P.O. Box 6121, 13083-862 Campinas, Brazil
[b] University of Campinas, P.O. Box 6121, 13083-862 Campinas, Brazil
[c] Fruit and Vegetable Technology Center, Institute of Food Technology, Brasil Avenue, 2880, P.O. Box 139, 13070-178 Campinas, Brazil
[d] Bakery and Confectionary Technology Center, Institute of Food Technology, Brasil Avenue, 2880, P.O. Box 139, 13070-178 Campinas, Brazil

ARTICLE INFO

Keywords:
Encapsulation
Anthocyanins
Hibiscus
Ionic gelation
Color

ABSTRACT

Hibiscus extract (HE) has a strong antioxidant activity and high anthocyanin content; it can be used as a natural pigment, also adding potential health benefits. The objective of this work was the microencapsulation of HE anthocyanin by ionic gelation (IG) using two techniques: dripping-extrusion and atomization, both by means of a double emulsion (HE/rapseed oil/pectin) and a cross-linked solution ($CaCl_2$). Particles (77–83% moisture content) were conditioned in acidified solution at 5, 15 and 25 °C, absence of light, and evaluated for anthocyanins and color for 50-days. The median diameter (D_{50}) of the particles ranged from 78 to 1100 μm and encapsulation efficiency ranged from 67.9 to 93.9%. The encapsulation caused higher temperature stability compared with the free extract. The half-life ($t_{1/2}$) values of the particles ranged from 7 (25 °C) to 180 days (5 °C) for anthocyanins and from 25 (25 °C) to 462 days (5 °C) for Chroma value. The IG increased the stability of HE anthocyanin. Both the dripping-extrusion and the atomization have shown to be feasible techniques.

1. Introduction

The use of plants as source of anthocyanins for phytonutrients and natural colorants has been studied by different authors (Mohd-Esa, Hern, Ismail, & Yee, 2010, Santos, Albarelli, Beppu, & Meireles, 2013; Da-Costa-Rocha, Bonnlaender, Sievers, Pischel, & Heinrich, 2014; Otálora, Carriazo, Iturriaga, Osorio, & Nazareno, 2016; Aizpurua-Olaizola et al., 2016).

Hibiscus (*Hibiscus sabdariffa* L.) is an herbaceous plant widely cultivated in tropical and subtropical areas of both hemispheres (Sinela et al., 2017). Its calyx can be used in the preparation of a slightly astringent and acid aqueous infusion. Geographical regions with tropical climate such as Sudan, Thailand, China, Mexico, Egypt, Senegal, and Tanzania are among the main commercial producers of this plant (Domínguez-Lopez, Remondetto, & Navarro-Galindo, 2008).

The hibiscus extract has antibacterial and antioxidant activity as well as hepatoprotective action, alleviating hunger and having effects on lipid metabolism (anti-cholesterol). It also has diuretic, anti-diabetic, anti-hypertensive effects, anti-inflammatory activities and other biological effects, such as cancer prevention and liver protection activities (Zhen et al., 2016). The presence of phenolic acids (especially protocatechuic acid), organic acids (hydroxycitric acid) and anthocyanins (delphinidin-3-sambubioside and cyanidin-3-sambubioside) may also contribute to the effects reported (Da-Costa-Rocha et al., 2014).

The ingestion of natural bioactive compounds, such as polyphenols and anthocyanins is of great interest, but the difficulties associated with the susceptibility of these compounds to adverse external effects, or damaging conditions of food processing and their chemical instability, have provided much effort to improve oral bioavailability. Therefore, microencapsulation represents a promising concept. The usage of microencapsulated bioactive compounds as functional ingredients in various food and beverage applications presents significant potential, as it may allow the enrichment of various food products with natural antioxidants (Diplock et al., 1999). Such ingredients are mainly wrapped in a wall material, thereby giving useful and/or eliminating useless properties of the original ingredient (Gharsallaoui, Roudaut, Chambin, Voilley, & Saurel, 2007).

In addition to being related to health benefits, such as antioxidants and anticancer agents, anthocyanins can be used as colorants. It is a water-soluble pigment and an alternative to the use of red to blue colors

* Corresponding author.
E-mail addresses: scmoura1@hotmail.com, smoura@ital.sp.gov.br (S.C.S.R. de Moura), carolberling@gmail.com (C.L. Berling), sgermer@ital.sp.gov.br (S.P.M. Germer), izabela@ital.sp.gov.br (I.D. Alvim), mhub@fea.unicamp.br (M.D. Hubinger).

http://dx.doi.org/10.1016/j.foodchem.2017.08.095
Received 8 May 2017; Received in revised form 25 August 2017; Accepted 28 August 2017
Available online 31 August 2017
0308-8146/

in foods (Reynertson et al., 2006). The replacement of artificial by natural colorants has gained consumer attention due to concerns about toxic and carcinogenic effects of artificial colorants and the growing search for healthy foods (Ko, Lee, Nam, & Lee, 2017). However, the use of anthocyanins is impaired by the instability of these molecules to adverse processing conditions and food storage. One of the ways of effectively protecting the anthocyanin compounds in the processed product is the microencapsulation.

Ionic gelation is a microencapsulation method that can be conducted by using atomization, dripping (coextrusion, extrusion), or electrostatic spray procedures. This method has the advantage of using mild conditions, since it does not employ high temperatures, vigorous stirring or organic solvents, enabling encapsulation of substances that would degrade under other conditions (Colak et al., 2016; Mukai-Corrêa, Prata, Alvim, & Grosso, 2005). A disadvantage is that encapsulation of hydrophilic or low molecular materials showed problems of easy diffusion and fast release through the ionic gel network regardless of pH (Kim, Lee, & Lee, 2016). Some strategies need to be applied (i.e. emulsion system, coating material) to retain the hydrophilic active compounds, since the ionic gelation has direct applicability for hydrophobic or low soluble active compounds only (Oehme, Valotis, Krammer, Zimmermann, & Schreier, 2011, Henning, Leick, Kott, Rehage, & Suter, 2012). The emulsion gelation technique using oil has been reported to create a barrier against the loss of hydrophilic compounds (Kim et al., 2016).

The ionic gelation technique for anthocyanin encapsulation was successfully used by several authors (Belscak-Cvitanovic et al., 2016; Santos et al., 2013; Yamdech, Aramwit, & Kanopanont, 2012). The unfavorable points shown by the authors when using this technique are the larger size and low stability of particles (mainly for hydrophilic active compounds). The favorable points are low polydispersity and good encapsulation efficiency. Macro and microparticles have been investigated in separate independent studies with different preparation conditions and core materials. Therefore, assessing the macro and microparticles with coherent conditions in a single study can reveal the characteristics of particles more clearly (Kim et al., 2016).

This work had the purpose of encapsulating the anthocyanin extract from hibiscus calyces by using a double emulsion and two ionic gelation methods (dripping – extrusion and atomization), as well as evaluating the stability of microcapsules at different storage temperatures.

2. Material and methods

2.1. Material

The following were used: food grade (30 g/100 g) hibiscus extract (*Hibiscus sabdariffa* L.) provided by *Heide Extratos Vegetais company*, Pinhais/PR; GENU® amidated low methoxyl pectin (CP Kelco, Limeira/SP); food grade calcium chloride (*Dinâmica*, Diadema/SP); rapeseed oil: commercial brand Liza oil (Cargill Agrícola S.A., Mairinque/SP); analytical grade reagents – PA and PGPR (polyglycerol polyricinoleate) surfactant (*Danisco Brasil Ltda*, Brazil).

2.2. Encapsulation of anthocyanin extract

In order to obtain hydrosoluble extract retention in gel matrix (also rich in water), a simple emulsion (w/o) was produced at first with rapeseed oil and PGPR surfactant (4 g/100 g) at a ratio of 35:65 w/w in ultra-turrax IKA T18 (15,000 rpm/15 min) disperser under controlled temperature (25 °C). Then a double emulsion (w/o/w) was produced with a pectin solution (2 g/100 g) in ultra-turrax IKA T18 (15,000 rpm/5 min) at a 20:80 w/w ratio.

2.2.1. Encapsulation by using dripping – extrusion method

Particles were produced using the Encapsulator equipment (Büchi B-390), nozzle diameter of 300 μm and air pressure of 200 mbar. The cross-linking solution was $CaCl_2$ (3 g/100 g). The following variables were considered on particle production: vibration frequency: 100–2200 Hz; electrode tension: 400–2000 V. The applied feed rate was 11.5 ml/min. The distance between the atomizer and the surface of $CaCl_2$ solution was 10 cm. The microspheres were stirred at 100 rpm for 15 min for hardening.

2.2.2. Encapsulation by atomization method

The particles were formatted by spraying, applying a double-fluid atomizer (mini spray dryer B-290 – nozzle 0.7 mm, adapted outside equipment), where double emulsion was sprayed on the cross-linking solution ($CaCl_2$ 3 g/100 g). For the experiments, the following variables were considered: air pressures ranging from 0.15 to 0.23 bar and feeding rates ranging from 0.70 to 1.61 ml/min. The distance between the atomizer and the surface of $CaCl_2$ solution was 18 cm. The microspheres were stirred at 100 rpm for 15 min for hardening.

2.3. Microparticles characterization

2.3.1. Mean diameter and size distribution

The samples had their mean diameters measured and size distribution determined in Laser Diffraction Analyzer LA-950V2 (Horiba Instruments, Inc., Japan) by using the liquid dispersion module with filtered water as dispersion medium. The mean diameter was expressed in two ways: based on the mean diameter of a sphere with the same volume (De Brouckere diameter – $D_{[4,3]}$), defined by Eq. (1), and median value (defined by the diameter that divides the population into two equal parts of 50% of accumulated volume) called D_{50}

$$D_{[4,3]} = \frac{\sum n_i d_i^3}{\sum n_i d_i^2} \quad (1)$$

where d_i is the diameter of particles and n_i is the number of particles.

The polydispersity index (PDI) was calculated according to Jafari, He, and Bhandari (2007), by using Eq. (2):

$$PDI = \frac{d_{90} - d_{10}}{d_{50}} \quad (2)$$

where d_{10}, d_{50} and d_{90} are the diameters at 10%, 50% and 90% of accumulated volume, respectively.

2.3.2. Color measurement

Colorimetric determinations were conducted by using Chromameter CR-400 (Konica-Minolta Sensing Inc., Osaka, Japan), programmed in CieLab system. The reading of color of particles was performed after the samples were filtrated in filter paper and put in Petri dishes. The readings were made in quadruplicate. Equipment was calibrated with the white calibration plate before any reading.

Chroma and hue values were also calculated by Eqs. (3) and (4).

$$Chroma = C^* = \sqrt{(a*^2 + b*^2)} \quad (3)$$

$$Hue = H^* = arctan\left(\frac{b*}{a*}\right) \quad (4)$$

2.3.3. Morphology

Particles morphology was analyzed according to the methodology adapted from Alvim, Souza, Koury, Jurt, and Dantas (2013), using an optical microscope (model BX41, brand Olympus) with 40X and 100X magnifications.

2.3.4. Moisture content

The moisture content was gravimetrically determined by drying at 70 °C with no vacuum for 24 h, followed by vacuum drying for additional 24 h. The analysis was made in triplicate, and approximately 10 g of the sample were weighed (AOAC., 2006).

2.3.5. Particles dissolution to bioactive quantifications

Particles obtained in better process conditions, that is, those with the best yields, lower polydispersion index (PDI) and higher values of chromaticity (C^*), have been chosen to bioactive compound extraction and quantification of anthocyanins, total polyphenols, and antioxidant capacity.

EDTA (0.2 M) under stirring (30 min) was used for particle dissolution at 10 g of wet particles. Then the extraction was conducted in Turratec Tecnal (Piracicaba, Brazil) model TE102 for 5 min, 4 times, with 2 × 20 mL with ethanol 70% and 2 × 20 mL with acetone 70%, alternately. At each wash, the sample was filtered into a grinding-mouth Erlenmeyer flask covered with aluminum foil and, in the last wash, the bioactive compound was transferred into a 100 mL volumetric flask covered with aluminum foil and stored protected from light, then being taken to quantification.

2.3.6. Content of total phenolic compounds

The total phenolics were determined according to the Folin-Ciocalteu spectrophotometric method described in Singleton and Rossi (1965) and used by Turkyilmaz, Tagi, Dereli, and Ozkan (2013). Absorbance readings (in triplicate) were made in UV/Visible spectrophotometer (Varian, model Cary 50). Microparticles without the bioactive compound were considered as control sample in order to disregard the effect of interfering substances on quantifications. An amount of 10 ± 0.01 g of sample was used (in triplicate).

2.3.7. Anthocyanin content

Total anthocyanins were determined by using the pH differential method, by AOAC (2006). Dilution was performed in a solution at pH 1 and 4.5, with quantification of absorbance on a wavelength of 520 and 700 nm in UV/Visible spectrophotometer (Varian, model Cary 50). The readings were made in triplicate. An amount of 5 ± 0.01 g of sample was used (in triplicate).

2.3.8. Antioxidant capacity

The antioxidant capacity by DPPH method was measured according to the Brand-Williams, Cuvelier, and Berset (1995) methodology and applied in Arend et al. (2017). Absorbance readings (in triplicate) were made in UV/Visible spectrophotometer (Varian, model Cary 50). An amount of 10 ± 0.01 g of sample was used (in triplicate).

2.3.9. Encapsulation efficiency (EE)

The amount of the bioactive compound effectively retained in microparticle structure after processing was measured. The encapsulation efficiency was calculated on wet basis by Eq. (5). This is important because it defines the amount of microparticles to be used (Kim, Lee, Oh, & Park, 2009).

$$\text{EE}\ (\%) = \frac{\frac{\text{mg of active in microparticle}}{\text{100 g}}}{\frac{\text{mg of active added in the mixture}}{\text{100 g mixture}}} \times 100 \quad (5)$$

The mixture was composed of: emulsion (rapeseed oil + hibiscus extract) + pectin solution.

2.3.10. FT – IR spectroscopic analysis

Equipment used was a Fourier transform infrared spectrophotometer – FT-IR, model IRPrestige-21 from the manufacturer Shimadzu (Kyoto, Japan) with data acquisition software: IRSolution, version 1.60.

Spectra of individual components (extract, pectin, and rapeseed oil) and microparticles were evaluated. Hibiscus extract and microparticles were previously dried in a vacuum oven at 70 °C for 24 h. The methodology adopted for particles, extract and pectin was KBr pressed disk technique (100:1 salt:sample w/w) and for rapeseed oil, the methodology applied was liquid film (KBr pastilles – 1 drop of sample). FI-IT spectra were collected in transmittance (%T) on a wavelength range of 400 to 4000 cm^{-1} with resolution of 4 cm^{-1}.

2.4. Anthocyanin storage stability studies

A stability study of the total anthocyanin content (AOAC, 2006) of microparticles and free hibiscus anthocyanin extract was conducted using climatic chambers model LS370-HUS-220 (Logen Scientific, São Paulo, Brazil) with 200-liter capacity. The free anthocyanin extract was stored at temperatures of 5 and 25 °C, in the absence of light and for a period of 55 days. The microparticles were stored at a high and constant humidity ($CaCl_2$ solution acidified at pH 3), at temperatures of 5, 15 and 25 °C, in the absence of light and for a period of 50 days. The color parameters CieLab were also evaluated and C^* (3), H^* (4) and ΔE (6) of microparticles were calculated.

$$\Delta E = \sqrt[2]{\Delta L^{*2} + \Delta a^{*2} + \Delta b^{*2}} \quad (6)$$

Kinetic models of degradation for each quality parameter assessed were obtained by evaluating the adjustments of model reactions of first order, as described by other authors (Moura et al., 2012; Nambi, Gupta, Kumar, & Sharma, 2016; Patras, Brunton, Tiwari, & Butler, 2011). The coefficient of determination of regression (r^2) was applied as a criterion to choose the best fit to experimental data, from which the reaction rate (k), half-life time ($t_{1/2}$), Q_{10} and activation energy (E) were obtained using Eqs. (7)–(10).

$$ln\left(\frac{C}{C_0}\right) = -kt \quad (7)$$

$$t_{1/2} = \frac{\ln 2}{k} \quad (8)$$

$$Q_{10} = \frac{k_T}{k_{T-10}} \quad (9)$$

$$Ea = 0{,}46 \times T^2 \times logQ_{10} \quad (10)$$

where T (Kelvin),Q_{10} (ΔT °C), E (cal. $g.mol^{-1}$)

2.5. Statistical methods

The results of the study were statistically evaluated using the analysis of variance (ANOVA) and Tukey's Test at the 5% level of significance, using the Statistica® software version 12 (StatSoft Inc., Tulsa, USA).

3. Results and discussion

3.1. Mean diameter and size distribution

Table 1 shows the results of mean diameter and size distribution of particles generated by dripping – extrusion and atomization techniques.

For particles generated by dripping, it can be observed that the increase in voltage and frequency had significant influence in the particle size reduction. In addition, Table 1 shows the higher difference in frequency and voltage values caused a reduction in microparticle size (about 30% of reduction), as well as a decrease in the PDI value (7.53% less).

The D_{50} values of microparticles generated by dripping-extrusion ranged from 788 to 1119 μm (Table 1). These values are smaller than the ones found by Eng-Seng, Zhin-Hui, Soon-Hock, Mansa, and Ravindra (2010) during encapsulation by dripping of aqueous herbal extract (2000 μm).

On the other hand, the D_{50} values are higher than the values (138.10–158.00 μm) obtained by Dorati, Genta, Modena, and Conti (2013), when they evaluated the microencapsulation of a hydrophilic model molecule (fluorescein) using the Buchi B-395 encapsulator and similar conditions of vibration frequency process (1600–2500 Hz) and

Table 1
Mean diameter and size distribution of microparticles.

Frequency/ Tension	Mean ($D_{4,3}$) (μm)	Median (D_{50}) (μm)	SD (sample)	PDI
Microparticles generated by dripping – extrusion				
100 Hz/400 V	1169.22a	1118.62a	311.33	0.598a
550 Hz/800 V	841.61b	802.54b	219.99	0.599a
1100 Hz/1200 V	904.46c	864.38c	235.75	0.590a
1650 Hz/1600 V	888.03c	847.38c	229.09	0.586a
2200 Hz/2000 V	888.10c	849.05c	224.50	0.563a
1100 Hz/2000 V	818.13d	788.33d	199.29	0.553b
Air pressure (bar)/ Feeding (ml/min)	Mean ($D_{4,3}$) (μm)	Median (D_{50}) (μm)	SD (sample)	PDI
Microparticles generated by atomization				
0.15/0.70	176.47 aA	165.03 aA	85.40	1.25 aA
0.15/0.93	225.02 dA	204.41 dB	120.81	1.42 dA
0.15/1.30	268.16 gB	246.59 gC	140.29	1.38 gB
0.15/1.61	303.36 jC	275.37 jC	158.84	1.38 jC
0.18/0.70	144.58 bA	77.56 bA	77.56	1.42 bA
0.18/0.93	188.18 eB	110.04 eB	110.04	1.57 eB
0.18/1.30	209.69 hC	129.28 hC	129.28	1.68 hC
0.18/1.61	212.32 kD	128.70 kC	128.70	1.65 kD
0.23/0.70	101.33 cA	78.20 cA	58.20	1.57 cA
0.23/0.93	106.95 fC	80.24 fB	70.24	1.92 fB
0.23/1.30	140.46 iA	90.93 iC	80.93	1.59 iA
0.23/1.61	126.31 lC	101.28 lBC	101.28	1.90 lB

Different letters in the same column indicate a significant difference ($p < 0.05$).
Small letters compare the differences in pressure under the same atomization feeding conditions.
Capital letters compare the differences in feeding under the same atomization pressure conditions.
SD – standard deviation.
PDI – polydispersity index.

electrode voltage from 1100 to 1900 V.

The results in Table 1 are in compliance with Aizpurua-Olaizola et al. (2016), who studied the variation of voltage, frequency and air pressure in Encapsulator Büchi B-390 to obtain particles rich in polyphenols from the residue of wine production. The results achieved by these authors showed that the best process conditions with the 300 μm nozzle were: high values of voltage (1150 Hz) and frequency (2000 V) and low values of air pressure (77 mbar), generating particles of 600 ± 90 μm. Under conditions of 1100 Hz, 2000 V and 200 mbar, D_{50} values of 788 μm were obtained in this work (Table 1).

For particles generated by atomization, increased air pressure at a given feeding rate has reduced the size of particles and increased the PDI. In addition, part of the sample became attached to the recipient wall that contains the cross-linking solution. The smaller size achieved was in 0.23 bar/0.70 ml/min condition, but yield was quite low.

The high feeding rates caused an increase in the particles median size (D_{50}), also causing an increase of PDI. The best process conditions were observed at air pressure values of 0.15 and 0.18 bar, and due to yield, the feeding rate of 1.30 ml/min has shown better values.

The size distribution of microparticles generated by dripping – extrusion was characterized by the monomodal behavior, with formation of a peak for larger particles (100 Hz/400 V – Table 1) close to 1100 μm, and for smaller particles (1100 Hz/2000 V – Table 1) close to 720 μm. The size distribution of microparticles generated by atomization was also characterized by the monomodal behavior, with the formation of a peak for larger particles (0.15 bar/1.61 ml/min – Table 1) close to D_{50} 275.37 μm and for smaller particles (0.23 bar/0.70 ml/min – Table 1) close to D_{50} 78.20 μm.

The median diameter of the microparticles in Table 1 falls among the D_{50} values (400 μm) of microparticles from the mulberry anthocyanin extract obtained by ionic gelation at different alginate concentrations (Yamdech et al., 2012).

The median diameter of the microparticles generated by dripping-extrusion (Table 1) was higher than for resveratrol microparticles (160.58–206.52 μm) obtained by ionic gelation using chitosan as core material and Encapsulator (B-390 Pro, Büchi) (Cho, Chun, Kim, & Park, 2014). In this study, the feeding of the emulsion in the Encapsulator required the use of a low pressure (200 mbar) and a 300 μm nozzle, which has consequently increased the microparticles size.

On the other hand, the results of D_{50} shown in Table 1 are lower than diameters of microparticles of polyphenolic compounds of dandelion (Taraxacum officinale L.) extract obtained by external gelation techniques with pectin as core materials (Belscak-Cvitanovic et al., 2016). These authors obtained D_{50} values ranging from 595 to 2250 μm and, in this work, the values ranged from 78 to 1100 μm.

According to Zhao, Sun, Torley, Wang, and Niu (2008), larger sized microparticles generally provide better protection than smaller ones, but dispersion is not good in food products. Selecting the particle size for appropriate application is important because particle characteristics determine its functionality in food matrices (Kim et al., 2016).

3.2. Analysis of color

For the dripping – extrusion method, the color analysis of the microparticles was conducted using different process conditions (Frequency/Tension) (Table 2).

At increased frequency and voltage, there is no significant difference in L^* (except to 1100 Hz/2000 V – Table 2), but there is a substantial difference in a^*, b^*, C^* and H^* from sample at 550 Hz/800 V. The highest values of C^* are found in particles generated at 100 Hz/400 V, which are also the biggest particles. Lowest C^* values are found in particles generated at 1100 Hz/2000 V, which are also the smallest particles. The condition of 1100 Hz/ 2000 V has generated particles with a significant difference in L^* (lighter), a^* (less red) and b^* (more yellow).

For the atomization method, the color analysis of the microparticles was also carried out for different process conditions (Air pressure/

Table 2
Color parameters of microparticles generated by dripping – extrusion and atomization techniques.

Frequency (Hz)/Tension (V)	L^*	a^*	b^*	C^*	H^*
Microparticles generated by dripping – extrusion					
100/400	53.16 a	24.46 a	5.78 a	25.137 a	0.232 a
550/800	50.16 a	21.38 b	5.16 b	21.997 b	0.237 ab
1100/1200	51.97 a	21.21 b	5.25 b	21.852 b	0.243 b
1650/1600	52.53 a	21.70 b	5.58 a	22.401 b	0.257 b
2200/2000	51.28 a	20.73 b	5.21 b	21.377 b	0.251 ab
1100/2000	54.29 b	16.28 c	4.02 c	16.769 c	0.242 b
Air pressure (bar)/ Feeding (ml/min)					
Microparticles generated by atomization					
0.15/0.70	64.63 aA	20.58 aA	3.77 aA	20.93 aA	0.18 aA
0.15/0.93	67.77 aAB	17.54 aB	4.08 aA	18.01 aB	0.23 aB
0.15/1.30	53.20 aC	25.62 aC	3.15 aB	25.81 aC	0.12 aC
0.15/1.61	70.34 aB	15.19 aD	4.68 aC	15.90 aD	0.30 aD
0.18/0.70	66.25 aA	18.03 bA	3.95 aA	18.46 bA	0.22 aA
0.18/0.93	70.26 aA	16.55 bB	4.67 bB	17.19 aA	0.27 bB
0.18/1.30	49.73 abB	23.62 abC	2.77 aC	23.78 abB	0.12 abC
0.18/1.61	66.24 bA	17.81 bAB	5.32 aD	18.59 bA	0.29 aA
0.23/0.70	56.21 bA	26.83 aA	2.96 bA	26.99 aA	0.11 aA
0.23/0.93	56.70 bA	26.63 cA	2.75 cA	26.77 bA	0.10 cA
0.23/1.30	56.60 acA	27.56 acA	3.01 aA	27.73 acA	0.11 bA
0.23/1.61	70.40 aB	15.42 aB	4.71 aB	16.12 aB	0.30 aB

Different letters in the same column indicate a significant difference ($p < 0.05$).
Small letters compare the differences in pressure atomization under the same feeding condition.
Capital letters compare the differences in feeding under the same pressure atomization condition.

Feeding rate) (Table 2).

As pressure has risen, a reduction in C^* and an increase in H^* up to a pressure of 0.18 were observed, followed by an increase in C^* and H^* at a pressure of 0.23 bar. The feeding value of 1.61 ml/min shows the worst conditions of color (the lowest C^* values) under all air pressure values, and a feeding value of 1.30 ml/min shows the best conditions of color (higher C^* values) under all air pressure conditions.

The larger particles obtained at process conditions of 0.15 bar/1.61 ml/min, showed lower values of C^* and higher values of H^*. The smaller particles, obtained at process conditions of 0.23 bar/0.70 ml/min, presented C^* and H^* values similar to those obtained at 0.23 bar/0.93 ml/min and 0.23 bar/1.30 ml/min.

The best process conditions for atomization system, that is, best yields, lowest PDI (particles without large differences in size) and highest C^* values (more saturated colors in the particles) were found at: air pressure of 0.15 bar and feeding of 1.30 ml/min and air pressure of 0.18 bar and feeding of 1.30 ml/min.

For the dripping – extrusion system, the studied conditions represent the process extremes, that is, conditions that generated the largest and smallest particles and the highest and lowest values of PDI and parameter C^*.

Therefore, microscopy and bioactive compounds analyses were conducted only in the following process conditions: dripping – extrusion: 100 Hz/400 V and 1100 Hz/2000 V and for atomization: air pressure of 0.15 bar and feeding of 1.30 ml/min and air pressure of 0.18 bar and feeding of 1.30 ml/min.

3.3. Microscopy

Fig. 1 shows the microstructure in stereoscope (magnification of 40x) of particles generated by dripping – extrusion, as well as the results of particles microscopy generated under the conditions of 100 Hz/400 V and 1100 Hz/2000 V by the dripping – extrusion method at a magnification of 100x and the results of particles microscopy generated under the conditions of 0.15 bar/1.30 ml/min and 0.18 bar/1.30 ml/min at a magnification of 100 and 1000x, by the atomization method.

For dripping –extrusion method at a magnification of 100x (Fig. 1B and C), several emulsion droplets were observed inside the microparticles, represented by the darkest portions.

Microparticles obtained in this study are irregular in spherical form as observed by Belscak-Cvitanovic et al. (2016) in their work with particles generated by external ionic gelation using pectin as core material. These authors showed lower regularity in spherical form for particles using pectin than particles using alginate as core material.

For atomization method at a magnification of 100x (Fig. 1D and F), several droplets of emulsion are observed inside the microparticles, represented by the darkest areas. At a magnification of 1000x (Fig. 1E and G), it can be observed some further details of emulsion droplets inside the particle, wrapped by the core material pellicle (pectin/$CaCl_2$ complex). Emulsion droplets are quite separated from each other, generating a free space and also exhibiting a considerable variation in size.

3.4. Moisture content

The moisture content of the microparticles was 83.07 ± 0.01% for dripping-extrusion and 77.03 ± 0.01% for those generated by atomization. These values are lower than those obtained by Belscak-Cvitanovic et al. (2016). The authors reported values of 92% water content for microparticles obtained by external gelation encapsulation in pectin hydrogels, probably due to a different microparticles composition.

3.5. Total phenolic compound content, anthocyanin content, and antioxidant capacity – Encapsulation efficiency

By using Eq. (5), the encapsulation efficiency (EE%) of bioactive compounds in microparticles generated by dripping – extrusion under the conditions of 100 Hz/400 V and 1100 Hz/2000 V were 74.4 and 88.5% for polyphenols, and 67.9 and 88.1% for anthocyanins. The maintenance of the antioxidant capacity was 55.2 and 60.6%. The smaller particles (1100 Hz/2000 V – Table 1) considering median diameter (D_{50}) had higher EE for all bioactive materials.

The encapsulation efficiency (EE%) of bioactive compounds in microparticles generated by atomization under the conditions of 0.15 bar/1.30 ml/min and 0.18 bar/1.30 ml/min was 80.0 and 95.6% for polyphenols and 84.3 and 93.9% for anthocyanins. The maintenance of the antioxidant capacity was 92.1 and 96.4%, which is considered high. The smaller particles (0.18 bar/1.30 ml/min – Table 1) considering median diameter (D_{50}) had higher EE for all bioactive materials.

Ionic gelation by atomization technique has shown better encapsulation efficiency, whereas smaller particles presented better encapsulation efficiency of bioactive compounds encapsulation.

Losses may occur during extraction due to contact with oxygen and exposure to light, characterized by lower stability of the extract under such conditions (Lopes, Xavier, Quadri, & Quadri, 2007).

The encapsulation efficiency (EE%) for anthocyanins in microparticles generated by atomization (84.3 and 93.9) was similar to those values presented by Santos et al. (2013), who reported the stability of *jabuticaba* peel extract by using supercritical solvent (80%) comparing to ionic gelation (Ca-alginate) by dripping (99%).

The maintenance of antioxidant capacity (55.2 and 60.6%) in microparticles generated by drip-extrusion was similar to that obtained by Hosseini et al. (2013) when studying a multiple/ionic emulsion method (o/w/o) for the production of alginate microparticles loaded with essential oil of Satureja hortensis (SEO). The encapsulation efficiency values obtained by these authors were in the range of 52–66%.

On the other hand, the maintenance of antioxidant capacity in microparticles generated by atomization (92.1 and 96.4%) was higher than the values (80–82%) demonstrated by Belscak-Cvitanovic et al. (2016) during the microencapsulation of dandelions by ionic gelation.

The EE values obtained in this study (55–96%) presented values higher than the ones obtained by Kim, Lee, & Lee, 2016. The authors reported values ranging from 29 to 41% when emulsion gelation techniques using sunflower oil to encapsulate catechins were applied.

3.5. Analysis of FT-IR spectroscopy

The analysis by FT-IR (Fig. 2) has enabled to distinguish the molecular interactions among respective microparticles components. For better visualization, the spectra of the compounds were separated as follows: microparticles generated by dripping – extrusion (A – particles and rapeseed oil, B – particles and extract and C – particles and pectin) and microparticles generated by atomization (D – particles and rapeseed oil, E – particles and extract and F – particles and pectin).

The IR spectrum of the microparticles consists of three different regions: (i) protein region (1700 and 1480 cm^{-1}) corresponding to C═O, C—N and N—H bonds, (ii) carbohydrate region (1200 and 870 cm^{-1}) related to absorption bands of C—O, C—C and C—O—H, and (iii) the region between 3500 and 2850 cm^{-1} attributed to O—H, N—H, C—H and C—H_2 bonds (Belscak-Cvitanovic et al., 2016).

The spectrum of rapeseed oil has two large peaks, which are shown in the region of 2924–2926 cm^{-1} (Point 1 of Fig. 2, A and D), attributed to the presence of —CH2 and 1743–1749 cm^{-1} (Point 2 of Fig. 2, A and D) assigned the C═O bonds. These results are in compliance with Zhen, Hong, and Dawei (2015), who evaluated the FT-IR absorption spectrum of rapeseed oil and found the highest peaks in 2919 cm^{-1} (asymmetrical stretching of —CH2) and 1747 cm^{-1} (—C═O stretching). These peaks are related to the presence of rapeseed oil in the microparticles.

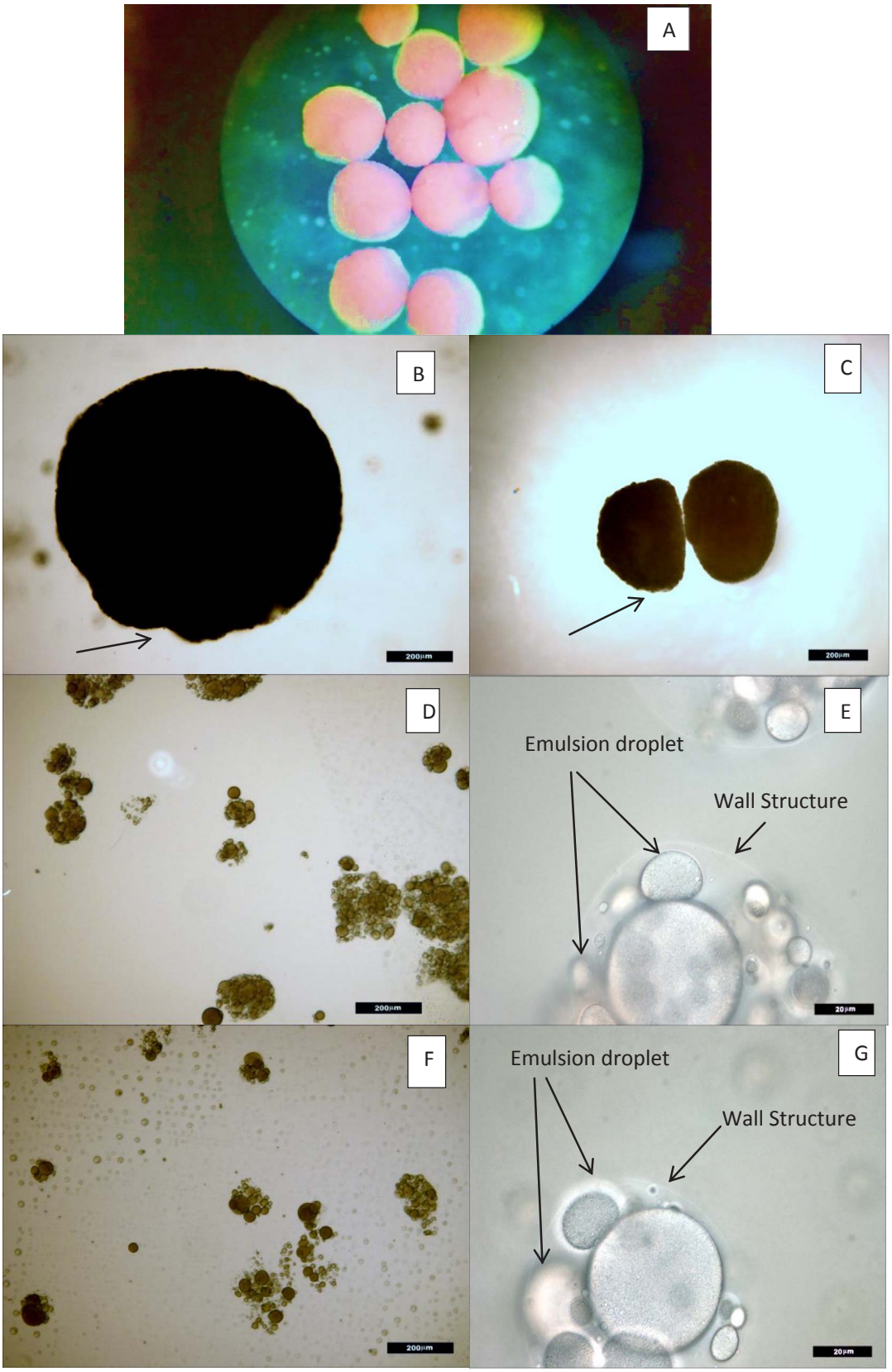

Fig. 1. Microstructure in stereoscope (magnification of 40x) (A) of particles generated by dripping – extrusion and in optical microscope under the conditions of 100 Hz/400 V (B) e 1100 Hz/2000 V (C) at a magnification of 100x. Microstructure of particles generated by atomization under the conditions of 0.15 bar/1.30 ml/min at a magnification of 100 (D) and 1000x (E) and under the conditions of 0.18 bar/1.30 ml/min at a magnification of 100 (F) and 1000x (G).

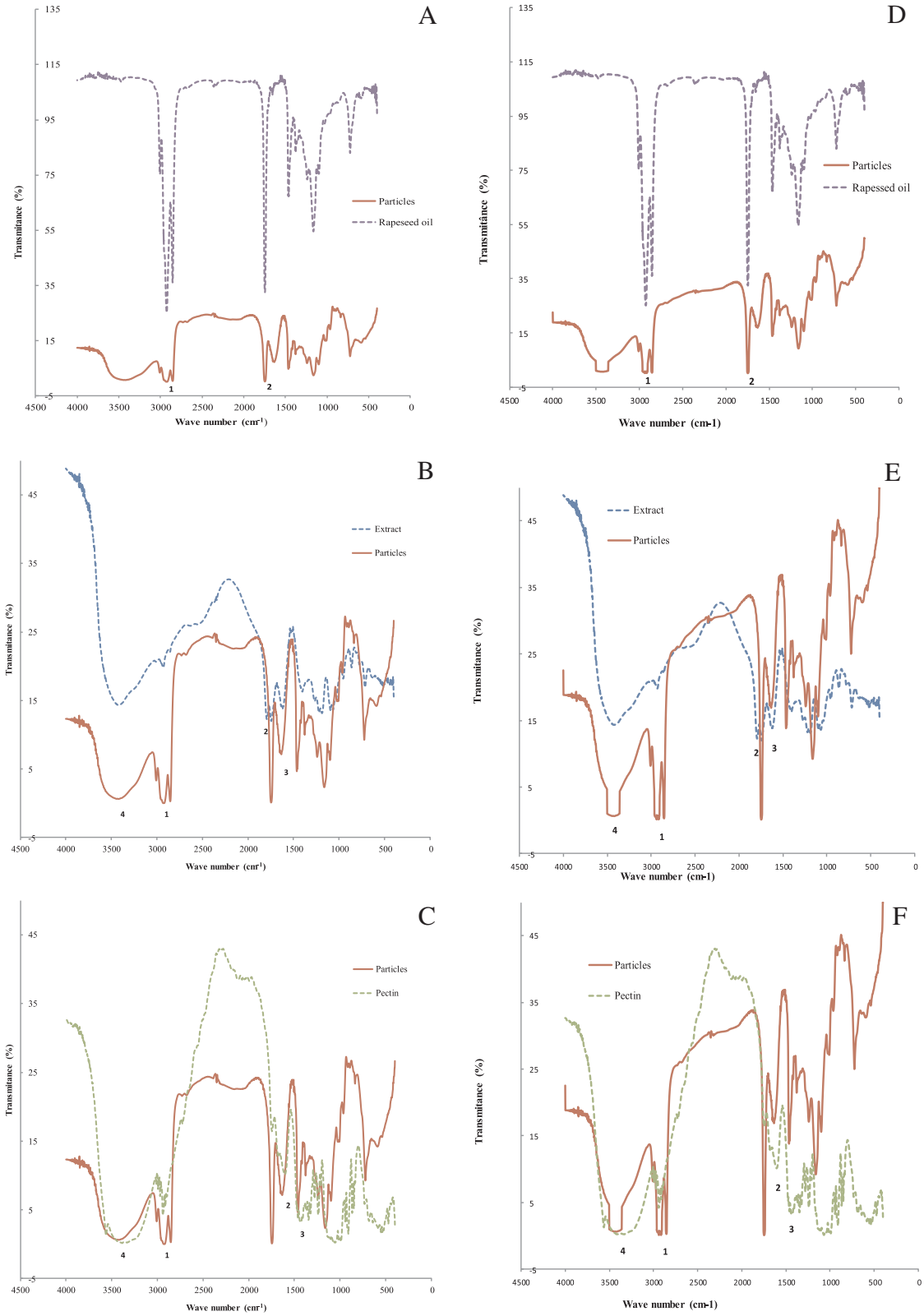

Fig. 2. FIT-IR spectrum of individual components and microparticles generated by dripping – extrusion: A – particles and rapeseed oil, B – particles and extract, C particles and pectin and spectrum of individual components and microparticles generated by atomization: D – particles and rapeseed oil, E – particles and extract, F particles and pectin.

The changes observed in hydroxyl and carbonyl regions in the spectrum of the microparticles containing hibiscus extract are a peak of O—H band (2926–3400 cm^{-1}), represented by point 1 of Fig. 2B, C, E and F, as well as a new peak in 1625–1637 cm^{-1}, represented by point 2 of Fig. 2B, C, E and F, which can be attributed to the interactions of hydrogen bonds with binding groups of active compounds and pectin. A slight spectral change in the region between 1317 and 1462 cm^{-1}, represented by point 3 of Fig. 2, B and E, can be imputed to the presence of hydroxycinnamic acids derived from hibiscus extract in microparticles.

In the microparticles spectrum, characteristic bands of groups present in the pectin structure are observed, with changes in intensity and displacement of some bands. The band in 3371–3496 cm^{-1}, represented by point 4 of Fig. 2B, C, E and F, refers to the O—H bonds stretching and is displaced to the lowest number of wave. It is also narrower, suggesting a potential interaction between the O—H groups of pectin and flavylium cation of the extract. Displacements and the change in intensity of the peak characteristic of the pectin group suggest a potential physical interaction between pectin and anthocyanin.

The symmetric COO^- deformation band around 1427 cm^{-1} in pectin shows a displacement of 1446–1462 cm^{-1}, represented by point 3 of Fig. 2, C and F in the microparticles curve, and its intensity is diminished. The band 1423–1427 cm^{-1} is specific to ionic bonding, and the binding of COO^- with the calcium ions from the cross-linking solution may modify charge density, atomic mass and the ray around the carbonyl groups, causing a displacement.

The presence of anthocyanin extract in microparticles was confirmed in this work by Fourier transform infrared spectroscopy (FT-IR) (Fig. 2). Likewise, Hosseini et al. (2013) studied a multiple emulsion method (o/w/o) for the production of alginate microparticles loaded with *Satureja hortensis* essential oil (SEO) and the presence of SEO in alginate microparticles was confirmed by Fourier transform infrared spectroscopy (FT-IR).

Specific interactions could be seen in Fig. 2 as Belscak-Cvitanovic et al. (2016) reported in a study of alginate and pectin microparticles formulated by ionic gelation of water in oil (w/o) emulsion. The FT-IR analysis of microparticles has shown specific interactions occurring between anthocyanin extract and core materials, with these being responsible for a better efficiency in capturing these compounds in particles formulated from binary mixtures.

3.6. Anthocyanin stabilization studies

A rise in anthocyanin degradation for free hibiscus anthocyanin extract (not encapsulated) was observed as the storage temperature increased (Fig. 3A). A similar behavior was described by Sinela et al. (2017) for degradation of major anthocyanins delphinidin-3-O-sambubioside and cyanidin-3-O-sambubioside in *Hibiscus Sabdariffa* extract.

Reaction kinetic models were applied to data and the best fits (higher r^2 values) were found for the first-order model. The kinetic parameters found after data adjustment where the reaction rate and activation energy (E) of 96.9 kJ/mol, calculated from Eq. (10), with $T = T_{ref} = 15\ ^\circ C = 288$ K and $Q_{10} = Q_{20}^{1/2} = (k_{25}.k_5^{-1})^{1/2} = 4.0$.

The value of activation energy was higher than the values presented by Cissé, Vaillant, Acosta, Dhuique-Mayer, and Dornier (2009) when they investigated the impact of temperature (30–90 °C) on degradation of anthocyanins for *roselle* extracts (47–61 kJ/mol). In compliance with this work, data of these authors show that thermal degradation of the anthocyanins can be described in terms of first order reaction kinetics.

The activation energy values for degradation of free hibiscus extract anthocyanin correspond to those values described by Sinela, et al. (2017), who observed E values of 90.0 ± 10.1 $kJ.mol^{-1}$ at a temperature ranged of 4–37 °C for degradation of major anthocyanin delphinidin-3-O-sambubioside and E of 80.0 ± 4.4 $kJ.mol^{-1}$ for degradation of major anthocyanin cyanidin-3-O-sambubioside in *Hibiscus Sabdariffa* extract.

With the purpose of evaluating the stability of total anthocyanin concentration (C) of microparticles generated by dripping – extrusion, a study was conducted at three temperatures: 5, 15 and 25 °C, in the absence of light, for the average period of 50 days.

Fig. 3B to E show the experimental results of anthocyanin degradation for microparticles generated by dripping – extrusion under conditions of 100 Hz/400 V and 1100 Hz/2000 V and anthocyanin degradation for microparticles generated by atomization under conditions of 0.15 bar/1.30 ml/min and 0.18 bar/1.30 ml/min.

The results showed that larger anthocyanin degradation was observed for particles generated at the 1100 Hz/2000 V condition (Fig. 3C) and at the 0.18 bar/1.30 ml/min condition (Fig. 3E), at the three storage temperatures, showing that the stability of anthocyanin in these particles (smaller diameters) was lower.

When stored at 5 °C, the microparticles showed a small change in anthocyanin content for 50 days. Anthocyanin retention was up to 97% after 35 days at 5 °C, 85% after 30 days at 15 °C and 26% after 20 days at 25 °C. The particles generated by dripping – extrusion showed degradation of anthocyanins approximately 16% lower than the particles generated by atomization when stored at 15 °C. At the temperature of 25 °C, the particles generated by the two ionic gelation techniques and under both process conditions showed a higher degradation of anthocyanins on the first 20 days of storage.

When these results were compared to those obtained by He et al. (2017), who evaluated the stability of nanoencapsulated anthocyanins in beverage model solution, data obtained in this study showed higher anthocyanin retention than the values obtained by these authors (84.5% after 35 days at 4 °C) and lower retention of anthocyanins after 12 days at 25 °C (68.4%). The impact of storage parameters (extrinsic) and microparticle composition (intrinsic) may have affected the stability of anthocyanins at different storage temperatures.

A temperature increase in the range of 5 up to 25 °C has caused $a\ L^*$ increase or a lightening, reduction of a^* or decrease of red color, increase of b^* or increase of yellow color, reduction of C^* or lower saturation, increase of H^* or change in shade and an increase in ΔE or color difference within the 50-day follow-up.

The anthocyanin and color degradation could be explained by a first-order kinetic model. Most literature data for change in food quality based either on destruction of pigments and vitamins during processing and storage, follow a first-order (n = 1) reaction model (Moura et al., 2012; Otálora et al., 2016, Aizpurua-Olaizola et al., 2016; Sinela et al., 2017; Ko, Lee, Nam, & Lee, 2017).

Table 3 shows the kinetic parameters found after data adjustment, where activation energy (E) was calculated from Eq. (10), with $T = T_{ref} = 15\ ^\circ C = 288$ K.

The increase in storage temperature has reduced the stability of anthocyanin and the color of the microparticles. The dripping – extrusion technique has generated particles with better stability of retention of anthocyanins and color, that is, smaller values of E and Q_{10} (Table 3).

When the anthocyanin degradation results of microparticles (Table 3) were compared with the degradation value of hibiscus anthocyanins extract, it was evidenced that encapsulation has led to a higher stability of anthocyanin, since the activation energy value found for the extract was E = 96.9 kJ/mol and $Q_{10} = 4.0$.

These results comply with those obtained by Yamdech et al. (2012), who studied the anthocyanin stability of blackberry extract with temperature change by using ionic gelation at different alginate concentrations (1.0–2.5%). The study demonstrated the encapsulation has increased the stability of anthocyanins in up to 40%. The study has also demonstrated that after exposure to 40 and 100 °C/10 h, the stability of anthocyanin was of 92% to 24%, respectively, showing the high degradation with temperature change of the microencapsulated anthocyanins.

The larger particles generated both by dripping – extrusion (100 Hz/400 V) and by atomization (0.15 bar/1.30 ml/min) had a longer half-life at 5 °C, ($t_{1/2}$ = 110 days; $t_{1/2}$ = 239 days) and lower E (32.0 kJ/mol; 49.59 kJ/mol) and Q_{10} (1.59; 2.0) regarding the anthocyanin content.

The results found in this study are in compliance with Zhao, Sun, Torley, Wang, and Niu (2008), who reported that larger microcapsules usually provide better protection than smaller ones, but could exhibit poor dispersion in final food products.

Although the encapsulation efficiency of smaller particles was higher, the stability of anthocyanin in these particles was lower.

The a^* and C^* parameters (Table 3) have the same temperature

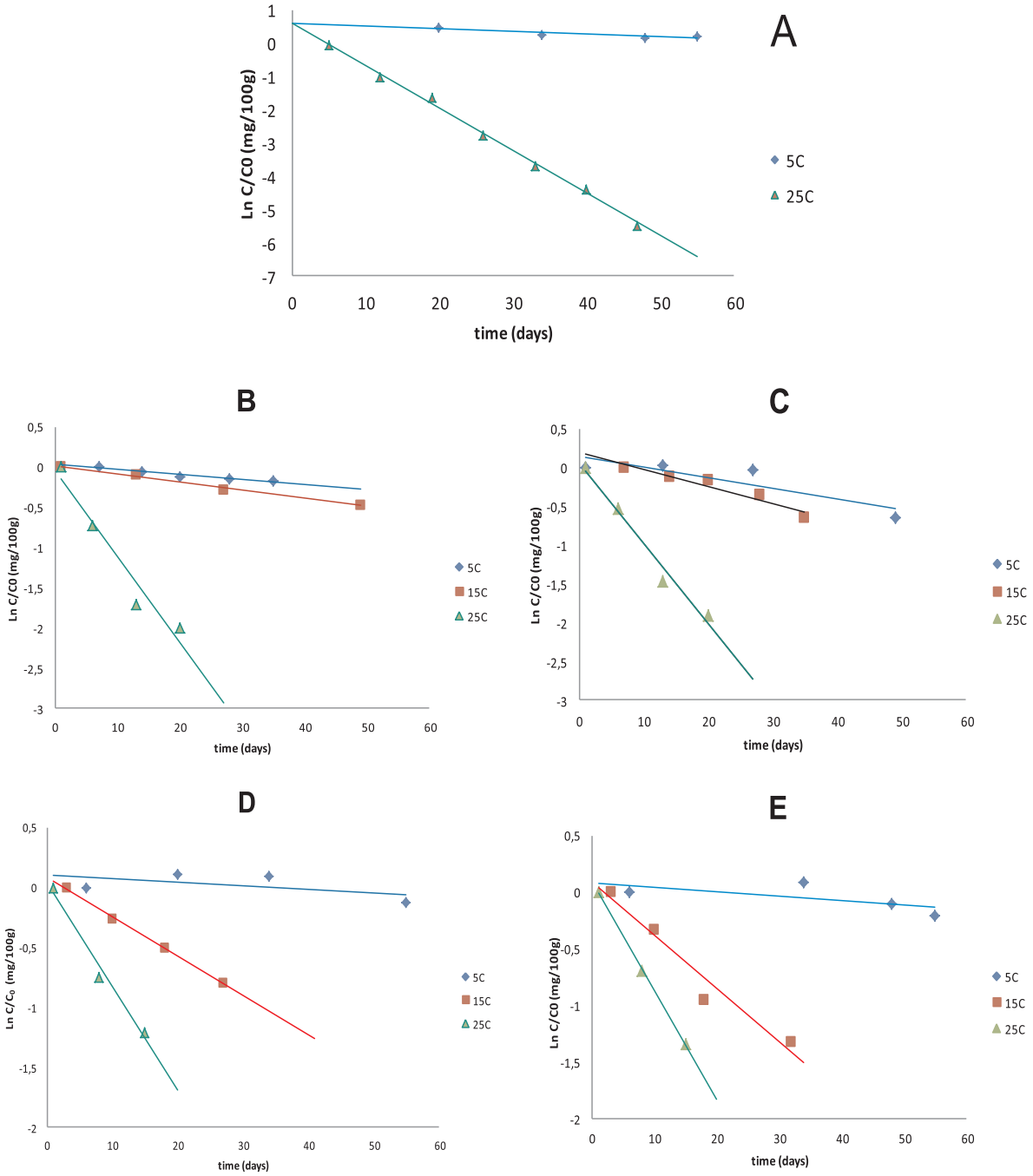

Fig. 3. Anthocyanin degradation in hibiscus extract (A); anthocyanin degradation in microparticles generated by dripping – extrusion under the conditions of 100 Hz/400 V (B) and1100 Hz/2000 V (C); and by atomization under the conditions of 0.15 bar/1.30 ml/min (D) and 0.18 bar/1.30 ml/min (E).

behavior as anthocyanin degradation, that is, larger particles exhibited lower degradation.

The microparticles obtained in this study were stored in acidified solution (pH 3.0) for the stability study. Likewise, the work developed by Santos et al. (2013) evaluated the stability of *jabuticaba* peel extract by using ionic gelation (Ca-alginate) method, and they concluded the anthocyanin extract encapsulated by ionic gelation showed higher stability in acid buffer solution.

The results achieved in this work have shown that even the microparticles with moisture content of 77–83% and stored at high moisture contents (acidified solution) had a good color stability and anthocyanin retention for at least 180 days ($t_{1/2}$) at 5 °C. When betalain was encapsulated using external ionic gelation and pigment stability in storage was evaluated at different humidity contents (34–84%) and temperatures (25 at 50 °C) for 25 days, Otálora et al. (2016) concluded that encapsulation provided a better protection of pigments than the non-encapsulated control material, with stability in storage being greater at a low relative humidity. In accordance with this work at a high relative humidity and temperature of 25 °C, there was no protection, and low storage stability was observed in the samples.

4. Conclusions

The ionic gelation method both by dripping – extrusion and atomization techniques has generated microparticles with high retention of anthocyanins without causing much degradation of the bioactive ingredients, showing to be feasible for stabilization of heat-sensitive compounds. With the atomization technique, smaller particles with

Table 3
Kinetic parameters of anthocyanin degradation and color of microparticles generated by dripping – extrusion under the conditions of 100 Hz/400 V (A) and 1100 Hz/2000 V (B), and by atomization under the conditions of 0.15 bar/1.30 ml/min (C) and 0.18 bar/1.30 ml/min (D).

Analyses	$k_{5°C}$ $(s)^{-1}10^{-7}$	$k_{15°C}$ $(s)^{-1}10^{-7}$	$k_{25°C}$ $(s)^{-1}10^{-7}$	$t_{1/2}$ 5 °C (days)	$t_{1/2}$ 15 °C (days)	$t_{1/2}$ 25 °C (days)	Q_{10}	E (kJ/mol)
Anthocyanin								
A	0.27	0.42	10.0	301.30	192.5	7.9	1.6	31.0
B	0.42	0.67	11.0	192.5	119.1	7.4	1.6	33.0
C	0,34	0,69	10,0	239,0	117,5	8,0	2,0	45,6
D	0,44	1,45	11,1	182,4	70,0	7,2	2,6	66,9
L^*								
A	0.06	0.07	0.25	1386.2	1155.2	315.0	1.2	12.6
B	0.07	0.17	0.37	1155.2	462.1	216.6	2.5	63.5
C	0.06	0.68	0.81	1386.2	117.5	99.0	11.8	171.1
D	0.01	0.29	0.50	6931.0	277.2	161.2	25.0	223.2
a^*								
A	0.07	0.35	1.90	1155.2	231.0	41.5	5.0	111.6
B	0.13	0.37	2.10	630.1	239.0	38.7	2.6	67.2
C	0.10	1.10	2.03	770.1	73.0	39.6	19.4	205.7
D	0.15	1.66	3.55	533.2	48.5	22.6	11.0	166.2
b^*								
A	0.06	1.20	1.47	1386.2	66.6	54.6	1.2	13.85
B	0.05	0.15	1.50	1732.8	462.1	53.3	3.3	81.7
C	0.59	0.57	0.97	135.9	141.4	82.5	1.0	27.7
D	0.82	0.17	0.31	97.6	462.1	256.7	1.8	40.75
C^*								
A	0.06	0.32	1.50	1386.2	247.5	53.3	5.6	119.4
B	0.13	0.32	1.60	630.1	247.5	49.9	2.5	64.8
C	0.12	1.83	3.13	693.1	43.9	25.7	15.8	191.3
D	0.17	1.55	3.26	462.1	51.7	24.6	8.9	151.8
H^*								
A	0.13	0.43	3.11	630.1	187.3	25.8	3.4	84.2
B	0.08	0.17	3.26	990.1	462.1	24.6	2.1	52.8
C	0.47	2.88	3.80	169.0	27.8	21.1	3.1	125.1
D	0.65	1.75	3.68	123.8	45.9	21.8	2.7	68.8
ΔE								
A	0.89	1.35	3.73	90.0	59.2	21.5	1.5	29.0
B	0.65	1.08	3.51	123.8	74.5	22.9	1.7	35.2
C	3.85	8.39	10.8	20.8	9.6	7.4	2.2	53.9
D	1.91	7.72	8.19	42.0	10.4	9.8	4.0	96.8

Correlation coefficient: $r^2 \geq 0.9$ (except for b^* parameter).
Where: k = reaction rate, ($t_{1/2}$) = half-life time $Q_{10}=\frac{k_T}{k_{T-10}}$ and E = activation energy.

better efficiency of bioactive compounds were obtained.

The encapsulation efficiency and antioxidant capacity were better for atomized particles however a greater stability was obtained for the particles produced by dripping – extrusion.

The increase in storage temperature has reduced the stability of anthocyanins and color of the microparticles. Anthocyanin degradation has followed the Arrhenius equation and we can affirm encapsulation promoted a higher stability with the temperature change compared with free hibiscus extract.

The encapsulation using dripping – extrusion technique at conditions of 100 Hz/400 V generated the lowest anthocyanin degradation at refrigerated storage.

Acknowledgments

The authors are grateful to the University of Campinas, Institute of Food Technology, FAPESP – Brazil (2009/54137-1) and CNPq – Brazil (PQ 304475/2013-0) for the financial support.

Appendix A. Supplementary data

Supplementary data associated with this article can be found, in the online version, at http://dx.doi.org/10.1016/j.foodchem.2017.08.095.

References

Aizpurua-Olaizola, O., Navarro, P., Vallejo, A., Olivares, M., Etxebarria, N., & Usobiaga, A. (2016). Microencapsulation and storage stability of polyphenols from *Vitis vinifera* grape wastes. *Food Chemistry, 190*, 614–621.

Alvim, I. D., Souza, F. S., Koury, I. P., Jurt, T. T., & Dantas, F. B. H. (2013). Use of the spray chilling method to deliver hydrophobic components: Physical characterization of microparticules. *Food Science and Technology, 33*(supl. 1), 34–39.

AOAC. (2006). Official Methods of Analysis of AOAC International. 18th ed. Maryland:AOAC International, 2006. Last revision 2010.

Arend, G. D., Adorno, W. T., Rezzadori, K., Di Luccio, M., Chaves, V. C., Reginatto, F. H., & Petrus, J. C. C. (2017). Concentration of phenolic compounds from strawberry (Fragaria X ananassa Duch) juice by nanofiltration membrane. *Journal of Food Engineering, 201*, 36–41.

Belscak-Cvitanovic, A., Busic, A., Barisic, L., Vrsaljko, D., Karlovic, S., Spoljaric, I., ... Komes, D. (2016). Emulsion templated microencapsulation of dandelion (Taraxacum officinale L.) polyphenols and β-carotene by ionotropic gelation of alginate and pectin. *Food Hydrocolloids, 57*, 139–152.

Brand-Williams, W., Cuvelier, M. E., & Berset, C. (1995). Use of a free radical method to evaluate antioxidant activity. *LWT – Food Science and Technology, 28*(1), 25–31.

Cho, A. R., Chun, Y. G., Kim, B. K., & Park, D. J. (2014). Preparation of chitosan–TPP microspheres as resveratrol carriers. *Journal of Food Science, 79*(4), 568–576.

Cissé, M., Vaillant, F., Acosta, O., Dhuique-Mayer, C., & Dornier, M. (2009). Thermal degradation kinetics of anthocyanins from blood orange, blackberry and roselle, using the Arrhenius, Eyring and Ball models. *Journal of Agriculture and Food Chemistry, 57*, 6285–6291.

Colak, N., Torun, H., Gruz, J., Strnad, M., Hermosín-Gutiérrez, I., Hayirlioglu-Ayaz, S., & Ayaz, F. A. (2016). Bog bilberry phenolics, antioxidant capacity and nutrient profile. *Food Chemistry, 201*, 339–349.

Da-Costa-Rocha, I., Bonnlaender, B., Sievers, H., Pischel, I., & Heinrich, M. (2014). *Hibiscus sabdariffa* L. – A phytochemical and pharmacological review. *Food Chemistry,*

165, 424–443.
Diplock, A. T., Aggett, P. J., Ashwell, M., Bornet, F., Fern, E. B., & Roberfroid, M. (1999). Scientific concepts of functional foods in Europe: Consensus document. *The British Journal of Nutrition, 81*, 1–27.
Domínguez-Lopez, A., Remondetto, G. E., & Navarro-Galindo, S. (2008). Thermal kinetic degradation of anthocyanins in a roselle (*Hibiscus sabdariffa* L. cv. "Criollo ") infusion. *International Journal of Food Science and Technology, 43*, 322–325.
Dorati, R., Genta, I., Modena, T., & Conti, B. (2013). Microencapsulation of a hydrophilic model molecule through vibration nozzle and emulsion phase inversion Technologies. *Journal of Microencapsulation, 30*(6), 559–570.
Eng-Seng, C., Zhin-Hui, Y., Soon-Hock, P., Mansa, R. F., & Ravindra, P. (2010). Encapsulation of herbal aqueous extract through absorption with ca-alginate hydrogel beads. *Food and Bioproducts Processing. 88*, 195–201.
Gharsallaoui, A., Roudaut, G., Chambin, O., Voilley, A., & Saurel, R. (2007). Applications of spray-drying in microencapsulation of food ingredients: An overview. *Food Research International, 40*, 1107–1121.
He, B., Ge, J., Yue, P., Yue, X. Y., Fu, R., Liang, J., & Gao, X. (2017). Loading of anthocyanins on chitosan nanoparticles influences anthocyanin degradation in gastrointestinal fluids and stability in a beverage. *Food Chemistry, 221*, 1671–1677.
Henning, S., Leick, S., Kott, M., Rehage, H., & Suter, D. (2012). Sealing liquid-filled pectinate capsules with a shellac coating. *Journal of Microencapsulation, 29*(2), 147–155.
Hosseini, S. M., Hosseini, H., Mohammadifar, M. A., Mortazavian, A. M., Mohammadi, A., Khosravi-Darani, K., ... Khaksar, R. (2013). Incorporation of essential oil in alginate microparticles by multiple emulsion/ionic gelation process. *International Journal of Biological Macromolecules, 62*, 582–588.
Jafari, S. M., He, Y., & Bhandari, B. (2007). Effectiveness of encapsulating biopolymers to produce sub-micron emulsions by high energy emulsification techniques. *Food Research International, 40*, 862–873.
Kim, E. S., Lee, J.-S., & Lee, H. G. (2016). Calcium-alginate microparticles for sustained release of catechin prepared via an emulsion gelation technique. *Food Science and Biotechnology, 25*(5), 1337–1343.
Kim, B. K., Lee, J.-S., Oh, J. K., & Park, D. J. (2009). Preparation of resveratrol-loaded poly (ε-caprolactone) nanoparticles by oil-in-water emulsion solvent evaporation method. *Food Science Biotechnology, 18*(1), 157–161.
Ko, A., Lee, J-S, Nam, H. S., & Lee, H. G. (2017). Stabilization of black soybean anthocyanin by chitosan nanoencapsulation and copigmentation. *Journal of Food Biochemistry, 41*. http://dx.doi.org/10.1111/jfbc.12316 e12316.
Lopes, T. J., Xavier, M. F., Quadri, M. G. N., & Quadri, M. B. (2007). Anthocyanins: A brief review of structural characteristics and stability. *Brazilian Journal of Agricultural Science, 13*(3), 291–297.
Mohd-Esa, N., Hern, F. S., Ismail, A., & Yee, C. L. (2010). Antioxidant activity in different parts of roselle (*Hibiscus sabdariffa* L.) extracts and potential exploitation of the seeds. *Food Chemistry, 122*, 1055–1060.
Moura, S. C. S. R., Tavares, P. E. R., Germer, S. P. M., Nisida, A. L. A. C., Alves, A. B., & Kanaan, A. S. (2012). Degradation kinetics of anthocyanin of traditional and low-sugar blackberry jam. *Food Bioprocess Technology, 5*, 2488–2496. http://dx.doi.org/10.1007/s11947-011-0578-7.
Mukai-Corrêa, R., Prata, A. S., Alvim, I. D., & Grosso, C. R. F. (2005). Characterisation of microcapsules containing casein and hydrogenated vegetable fat, obtained by ionic gelation. *Brazilian Journal of Food Technology, 8*(1), 73–80.
Nambi, V. E., Gupta, R. K., Kumar, S., & Sharma, P. C. (2016). Degradation kinetics of bioactive components, antioxidant activity, colour and textural properties of selected vegetables during blanching. *Journal of Food Science and Technology*. http://dx.doi.org/10.1007/s13197-016-2280-2.
Oehme, A., Valotis, A., Krammer, G., Zimmermann, I., & Schreier, P. (2011). Preparation and characterization of shellac-coated anthocyanin pectin beads as dietary colonic delivery system. *Molecular Nutrition & Food Research, 55*, S75–S85.
Otálora, M. C., Carriazo, J. G., Iturriaga, L., Osorio, C., & Nazareno, M. A. (2016). Encapsulating betalains from *Opuntia ficus-indica* fruits by ionic gelation: Pigment chemical st during storage of beads. *Food Chemistry, 202*(1), 373–382.
Patras, A., Brunton, N. P., Tiwari, B., & Butler, F. (2011). Stability and degradation kinetics of bioactive compounds and colour in strawberry jam during storage. *Food Bioprocess Technology, 4*, 1245–1252.
Reynertson, K. A., Wallace, A. M., Adachi, S., Gil, R. R., Yang, H., Basile, M. J., ... Kennelly, E. J. (2006). Bioactive despised and anthocyanins from jabuticaba (*Myrciaria cauliflora*). *Journal of Natural Products, 69*(8), 1228–1230.
Santos, D. T., Albarelli, J. Q., Beppu, M. M., & Meireles, M. A. A. (2013). Stabilization of anthocyanin extract from jabuticaba skins by encapsulation using supercritical CO2 as solvent. *Food Research International, 50*, 617–624.
Sinela, A., Rawat, N., Mertz, C., Achir, N., Fulcrand, H., & Dornier, M. (2017). Anthocyanins degradation during storage of *Hibiscus sabdariffa* extract and evolution of its degradation products. *Food Chemistry, 214*, 234–241. http://dx.doi.org/10.1016/j.foodchem.2016.07.071.
Singleton, V. L., & Rossi, J. A. (1965). Colorimetry of total phenolics with phosphomolybdic-phosphotungstic acid reagents. *American Journal of Enology and Viticulture, 16*(3), 144–158.
Turkyılmaz, M., Tağı, S., Dereli, U., & Ozkan, M. (2013). Effects of various pressing programs and yields on the antioxidant activity, antimicrobial activity, phenolic content and color of pomegranate juices. *Food Chemistry, 138*, 1810–1818.
Yamdech, R., Aramwit, P., & Kanopanont, S. (2012). Stability of anthocyanins in mulberry fruit extract adsorbed on calcium alginate beads. *1a. Mae Fah Luang University International Conference*, 1–8.
Zhao, R., Sun, J., Torley, P., Wang, D., & Niu, S. (2008). Measurement of particle diameter of Lactobacillus acidophilus microcapsule by spray drying and analysis on its microstructure. *World Journal of Microbiology Biotechnology and Biotechnology, 24*(8), 1349–1354.
Zhen, W., Hong, L., & Dawei, T. (2015). Application of Fourier transform infrared (FT-IR) spectroscopy combined with chemometrics for analysis of rapeseed oil adulterated with refining and purificating waste cooking oil. *Food Analytical Methods, 8*, 2581–2587.
Zhen, J., Villani, T. E., Guo, Y., Qi, Y., Chin, K., Pan, M.-H., ... Wu, Q. (2016). Phytochemistry, antioxidant capacity, total phenolic content and anti-inflammatory activity of *Hibiscus sabdariffa* leaves. *Food Chemistry, 190*, 673–680.